

Comb and Bottlebrush Polymers with Superior Rheological and Mechanical Properties

Mahdi Abbasi,* Lorenz Faust, and Manfred Wilhelm

Comb and bottlebrush polymers present a wide range of rheological and mechanical properties that can be controlled through their molecular characteristics, such as the backbone and side chain lengths as well as the number of branches per molecule or the grafting density. This review investigates the impact of these characteristics specifically on the zero shear viscosity, strain hardening behavior, and plateau shear modulus. It is shown that for a comb polymer with an entangled backbone and entangled side chains, a maximum in the strain hardening factor and minimum in the zero shear viscosity η_0 can be achieved through selection of an optimum number of branches q . Bottlebrush polymers with flexible filaments and extremely low plateau shear moduli relative to linear polymers open the door for a new class of solvent-free supersoft elastomers, where their network modulus can be controlled through both the degree of polymerization between crosslinks, n_x , and the length of the side chains, n_{sc} , with $G_{BB}^0 \approx \rho k T n_x^{-1} (n_{sc} + 1)^{-1}$.

1. Introduction

Comb polymers are a class of branched polymers consisting of a linear backbone with a low grafting density of side chains,^[1] while bottlebrushes are formally also combs but with a significantly higher grafting density of the side chains.^[2,3] These classes of polymers can be synthesized via different polymerization techniques, e.g., anionic polymerization,^[1,4,5] ring-opening metathesis polymerization (ROMP),^[6] atom transfer radical polymerization (ATRP),^[7] and reversible addition–fragmentation chain transfer (RAFT),^[8] combined with a grafting method: grafting-from, grafting-to, and grafting-through.^[3,9] Systematic investigation of different relaxation times and plateau modulus of these polymers ideally requires monodisperse systems with well-entangled backbone and side chains as well as well-defined number of branches per backbone (or grafting density) with equal branching point spacing. The anionic polymerization

combined with the grafting-to method^[1,10] results in comb polystyrenes (PSs) with well-entangled monodisperse backbone and side chains; however, branch points along the backbone are randomly distributed. This random distribution of branch points has no distinct effect on the rheological properties of dense comb topologies; however, it will broaden the backbone relaxation time of loose comb topologies even though the molecular weight distribution is narrow enough.^[11] A controlled branching point spacing can be achieved through the coupling of living macroanions;^[12] however, this method is prone to slightly high molecular weight distribution, $\mathcal{D} > 1.5$. Synthesis of well-defined densely grafted bottlebrushes using ROMP and grafting-through method

guarantees the presence of one side chain per repeating unit on the backbone. Bottlebrushes with more than one branch per backbone repeating unit can also be synthesized using ROMP and macromonomers with more bulky groups referred as wedge polymers.^[13] These bottlebrushes are similar to that of the dendronized polymer with only one layer of grafting. Loosely grafted bottlebrushes with longer distance between the branching points can be achieved using ROMP technique through copolymerization of macromonomer and a diluent molecule, e.g., racemic endo,exo-norbornenyl diesters, with different ratios. However, different reactivity of macromonomer and diluent leads to a gradient of branching point spacing along the backbone,^[14] where the conformations of side chains along the backbone are affected by this gradient.^[15] It should be mentioned that the bottlebrushes synthesized with ROMP technique have different repeating units in the backbone than the side chains which might cause microphase separation. However this issue could be ignorable in dense bottlebrushes where the volume fraction of backbone is less than 1 wt%. In order to avoid any microphase separation, Sheiko and co-workers^[16] synthesized a series of dense combs and loose bottlebrushes homo poly(*n*-butyl acrylates) (PBA) with similar side chains and systematically varied grafting density through copolymerization of nonfunctional *n*-butyl acrylates with trimethylsilyl-protected acrylates by ATRP. However, in order to achieve high degree of polymerization (DP) of backbone (entangled system) for dense bottlebrushes, they had to use slightly different backbones, i.e., poly(*n*-butyl methacrylate). An organometallic coordinative insertion polymerization of α -olefins results in entangled densely grafted bottlebrushes with rod-like side chains where both backbone and side chains have alkane groups. However the dispersity index of such homopolymer bottlebrushes would

Dr. M. Abbasi,^[†] L. Faust, Prof. M. Wilhelm
Institute of Chemical Technology and Polymer Chemistry
Karlsruhe Institute of Technology (KIT)
Engesserstraße 18, 76131 Karlsruhe, Germany
E-mail: mahdi.abbasi@partner.kit.edu, mahdi.abbasi@borealisgroup.com

 The ORCID identification number(s) for the author(s) of this article can be found under <https://doi.org/10.1002/adma.201806484>.

^[†]Present address: Borealis Polyolefine GmbH, Innovation Headquarters, 4021, Linz, Austria

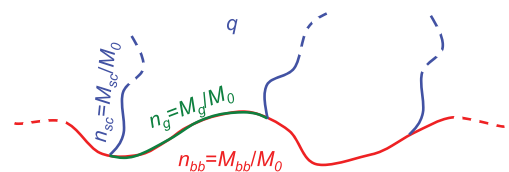
© 2019 The Authors. Published by WILEY-VCH Verlag GmbH & Co. KGaA, Weinheim. This is an open access article under the terms of the Creative Commons Attribution-NonCommercial License, which permits use, distribution and reproduction in any medium, provided the original work is properly cited and is not used for commercial purposes.

DOI: 10.1002/adma.201806484

be around $\mathcal{D} \approx 2$.^[17–19] In addition, the glass transition temperature of the comb and bottlebrush topologies depends on the length of branches as well as their polarity.^[18,20,21] All of these synthetic constraints and inherent properties should be considered in generic conclusions for rheological data linked to the polymer physics.

Viscoelastic characteristics as described by the rheological and mechanical properties of comb and bottlebrush polymers strongly depend on the formation of entanglements as well as the backbone and side chain conformations.^[3,10,22–28] A comb structure can be quantified through three independent molecular characteristics: the molecular weight of the backbone, M_{bb} , the molecular weight of the side chains, M_{sc} , and the number of side chains per backbone, q . However, M_{bb} and M_{sc} of the comb structures mostly are normalized to the molecular weight between physical entanglements, M_e , which are referred to as the number of entanglements in the backbone, $Z_{bb} = M_{bb}/M_e$, and the number of entanglements in the side chain, $Z_{sc} = M_{sc}/M_e$, respectively. It should be mentioned that here M_e is a constant for a given chemical composition and for simplicity is defined as an entanglement strand of a linear polymer of the same chemical composition as its comb (or bottlebrush) counterpart. Another dependent molecular characteristic for comb topologies is the average number of entanglements between the branching points, $Z_g = Z_{bb}/(q + 1)$. The molecular weight of backbone, M_{bb} , and side chains, M_{sc} , of bottlebrush structures are normalized to the monomer molecular weight, M_0 , as the DP of the backbone, $n_{bb} = M_{bb}/M_0$, and DP of the side chain, $n_{sc} = M_{sc}/M_0$. Nevertheless, the average DP between two neighbor branching points, $n_g = M_g/M_0$, or the grafting density, n_g^{-1} , together with the DP of the side chains, n_{sc} , are often used for bottlebrush polymers (see **Figure 1**). In the current paper, we investigate the transitions from comb to bottlebrush behavior; therefore, all of these variables are used for both topologies especially in the transition from comb to bottlebrush conformations. **Figure 1** shows the correlation between these variables.

Substantial experimental^[11,29–31] and coarse-grained simulation works along with scaling analysis^[24,25,32–35] have been done to classify graft polymers into comb and bottlebrush classes with distinct rheological and mechanical properties. The differences observed between comb and bottlebrush structures were related to the Gaussian and stretched conformations of the backbone and side chains.^[24,25] Comb topologies have a backbone and side chains with an unperturbed random Gaussian conformation, while a densely grafted bottlebrush has a stretched backbone and side chains. The side chains of the comb topologies can easily overlap physically with each other, while densely grafted bottlebrush molecules are segregated and weakly penetrated.



	Backbone	Side chain	Branch point spacing
Molecular weight	M_{bb}	M_{sc}	M_g
Degree of polymerization	$n_{bb} = M_{bb}/M_0$	$n_{sc} = M_{sc}/M_0$	$n_g = M_g/M_0$ or $n_g = n_{bb}/(q+1)$
Number of entanglements	$Z_{bb} = M_{bb}/M_e$	$Z_{sc} = M_{sc}/M_e$	$Z_g = M_g/M_e$ or $Z_g = Z_{bb}/(q+1)$
Volume fraction	$\phi_{bb} = M_{bb}/(M_{bb} + qM_{sc})$	$\phi_{sc} = 1 - \phi_{bb}$	-

Figure 1. Molecular characteristics of comb and bottlebrush polymers.



Mahdi Abbasi is a postdoctoral fellow in the Institute for Chemical Technology and Polymer Chemistry at Karlsruhe Institute of Technology (KIT), Germany. He obtained his Ph.D. degree from Tarbiat Modares University, Iran, in 2012. He worked as a Humboldt fellow at KIT on the foaming and rheology of model comb and bottlebrush polymers.



Manfred Wilhelm is a professor in the Institute for Chemical Technology and Polymer Chemistry at Karlsruhe Institute of Technology, Germany. One of his research interests is method development using rheological-based combined techniques for the characterization of branched topologies.

Side chains were introduced on comb polymers to mainly control the rheological properties of polymers melt and solutions, especially the extensional viscosity and strain hardening behavior under extensional deformations, through variation of Z_{bb} , Z_{sc} , and q .^[10,11,22,36–43] While bottlebrushes generally were designed to control the elastic properties of polymers, e.g., the shear and extensional moduli, through independent variation of the DP of side chain, n_{sc} , and their grafting density, n_g^{-1} .^[3,24,25,32,44] Side chains in comb polymers increase the friction of the backbone chain with neighboring molecules in the melt or solution state, which enhances the strain hardening (see below) of the polymer melt under processing conditions. Consequently, entangled side chains induce substantially higher strain hardening than unentangled branches in comb polymers due to their higher topological constraint. However, both the shear and extensional viscosity increase exponentially^[22,35,38,45] with the length of the entangled branches, which results in ultrahigh viscous materials with poor processing properties. Therefore, an optimum length of entangled branches is assumed to exist for comb polymers to improve the practically

very important strain hardening properties. According to the experimental and theoretical results on comb polymers with entangled branches, the strain hardening properties exponentially increase with side chain length, while glassy modulus and arm relaxation plateau modulus are weakly affected by the well-entangled side chains. However, rubbery plateau modulus related to the backbone relaxation time reduces (dilutes) by decreasing of volume fraction of backbone, $G_{N,s}^0 = G_N^0 \phi_{bb}^{1+\alpha}$. The self-dilution effect of side chains in comb polymer melts is different than the dilution concept in polymer solution due to the simultaneous strong frictional role of side chains in comb polymer melts compared to the frictional effect of unentangled solvent molecules in polymer solutions. In the current progress report, we investigate the behavior of the comb and bottlebrush topologies only in the melt state.

Side chains in bottlebrushes suppress the entanglement threshold of polymer strands, which reduces the rubber plateau modulus from typically 1 MPa for an entangled linear polymer down to 100 Pa for a densely grafted bottlebrush polymer. This substantial reduction in both entanglements and modulus creates the possibility to design supersoft and at the same time superelastic elastomers^[46–48] which have a tensile strain at break up to 800% in the solvent-free networks.^[24] Densely grafted bottlebrushes are supposed to be thick (compare to linear polymer), flexible, cylindrically shaped filaments with both stretched side chains and backbone due to the steric repulsion between densely grafted side chains. Therefore, the side chains of a given bottlebrush molecule cannot interpenetrate the pervaded volume of side chains of neighboring molecules. This means that longer side chains in bottlebrushes theoretically result in a bigger diameter for a given polymer strand and, therefore, a lower modulus, $G_N^0 \propto M_e^{-1}$. However, increasing the length of a side chain above the entanglement length of a linear polymer increases the pervaded volume of the end of the side chains where they can penetrate among the side chains of neighboring molecules and possibly make more entanglements. Therefore, the relaxation time of loosely grafted bottlebrushes with entangled side chains drastically increases, which results in ultrahigh zero shear viscosity.^[11]

Figure 2 shows the difference between the comb and bottlebrush structures according to their main applications. Figure 2a–c shows that branched polymers which have mainly comb topology are mostly used in extensional, e.g., electrospinning^[28] and foaming, processes where their strain hardening properties under uniaxial and biaxial extensional deformations are of great importance, respectively. Electrospinning of three different comb polystyrene solutions with the same backbone, $M_{n,bb} = 90 \text{ kg mol}^{-1}$, and similar volume fraction of side chains $\phi_{sc} \approx 0.64$, showed that transition in morphology of electrospun fibers from bead to fiber structure occurred at substantially lower polymer concentrations for combs with fewer, but longer side chains.^[28] The current research in our group on a series of comb PS with the same backbone, $M_{w,bb} = 290 \text{ kg mol}^{-1}$, and similar side chains, $M_{n,sc} = 44 \text{ kg mol}^{-1}$, but different number of side chains per backbone showed that a comb with 120 side chains, PS290-120-44, shows the maximum strain hardening and minimum zero shear viscosity in this series.^[11] The scanning electron microscopy image in Figure 2a is related to

the foam of this comb PS with a cell density of $10^9 \text{ cells cm}^{-3}$, volume expansion ratio around 40, and an average wall thickness of the cells around 250 nm. In the other word, the lower zero shear viscosity of a comb structure facilitates the bubble growing at the early stage of foaming, while the higher strain hardening property of comb PS stabilizes the ripened cells at the end of foaming process. To the best of our knowledge, there is no available biaxial extensional data for well-defined comb or bottlebrush polymers; however, commercial branched polymers showed strain hardening under biaxial extension.^[49,50] In Section 2, we investigate the effect of different molecular characteristics, Z_{bb} , Z_{sc} , and q , on the shear and extensional viscosity as well as strain hardening behavior. The impact of each characteristic specifically on the zero shear viscosity behavior, η_0 , and the strain hardening factor (SHF), $\text{SHF} \approx \eta_E^{\text{max}}/3\eta_s$, will be clarified by reviewing the literature on experimental and modified reptation-based models for comb topologies.

Matyjaszewski and co-workers^[51] recently reviewed the correlations between bottlebrush architectures and their properties as novel materials with various potential applications such as templates of well-defined nanostructures, drug carriers, surfactants, lubricants, stimuli-responsive materials, and supersoft elastomers. Figure 2d–f shows the advantages of using bottlebrush elastomers as solvent-free, supersoft, and superelastic materials compared with hydrogels and conventional elastomers.^[24,44] One example is that a poly(dimethylsiloxane) (PDMS) bottlebrush elastomer exhibits a considerably higher fracture energy than its poly(acrylamide) (PAM) hydrogel counterpart with a similar backbone volume fraction (Figure 2d,e), even though both materials show a similar modulus. Moreover, bottlebrush elastomers exhibit substantially higher compression ratios at break, ≈ 10 , relative to hydrogels, ≈ 3 . Comparison of true stress as a function of areal expansion ($\sigma_{\text{true}} - \lambda^{-1}$) for a conventional elastomer and a bottlebrush elastomer (Figure 2f) shows that a conventional elastomer (line 1) with coiled network strands exhibits linear elasticity over a wide range of areal expansion without strain-stiffening (increase in modulus during deformation) properties. Prestretching and then bracing these conventional elastomers with either physical (e.g., lamination) or chemical (swelling in a solvent) methods results in materials with better strain-stiffening properties (line 2), which is necessary for the use of dielectric elastomers in an actuator application. However, these kinds of modifications to dielectric elastomers increase the size of the total actuator assembly leading to a significant reduction in efficiency.^[44] Bottlebrush elastomers (line 3) with an inherently prestrained structure have inherent strain-stiffening properties as a single component. Furthermore, polymer chains in bottlebrush elastomers are disentangled, which results in high extensibility. In Section 3, the effect of the different molecular characteristics of bottlebrush elastomers, n_{sc} and n_g , as well as degree of polymerization of backbone between crosslinks, n_x , on the plateau modulus are presented. Transitions from a comb topology with unperturbed backbone and side chain conformations to a loosely grafted bottlebrush with a stretched backbone conformation and finally to a densely grafted bottlebrush with both stretched backbone and side chains will be discussed in more detail.

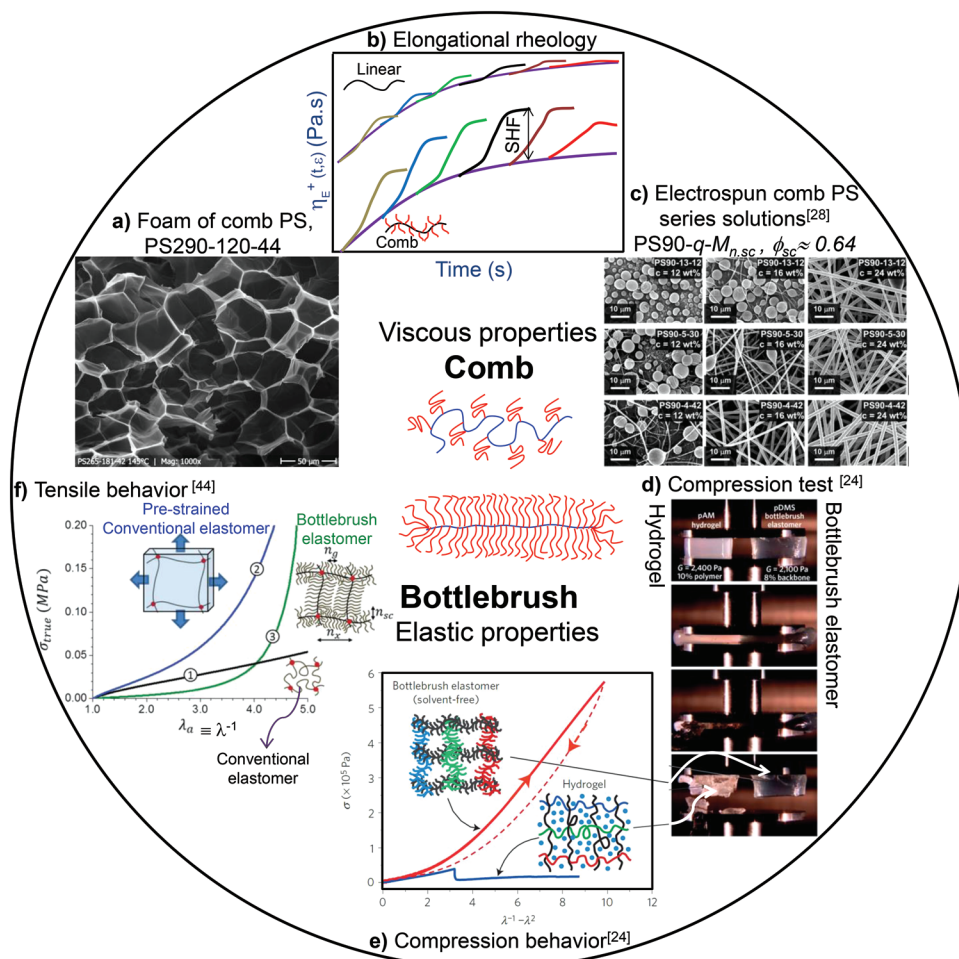


Figure 2. Classification of comb and bottlebrush structures according to their applications. Comb polymers are mainly used in processes which are based on the extensional deformation of polymers with pronounced strain hardening compared to the linear polymers (b). c) Transition from bead to fiber morphology as a function of concentration of electrospun solutions (12, 16, 24 wt%) of three different comb PS, abbreviated PSM_{n,bb}-q-M_{n,sc}, which have the same backbone, M_{n,bb} = 90 kg mol⁻¹, and similar volume fraction of side chains $\phi_{sc} \approx 0.64$, but different number, *q* = 13, 5, 4, and molecular weight, M_{n,sc} = 12, 30, 42 kg mol⁻¹, of side chains. Reproduced with permission.^[28] Copyright 2016, Elsevier. a) Foam out of a comb PS290-120-44 which results in a foam structure with cell density of 10⁹ cells cm⁻³, volume expansion ratio around 40, and an average wall thickness of the cells around 250 nm. Bottlebrush polymers (d–f) are used as bottlebrush elastomers with solvent-free, supersoft, and superelastic properties. d) Compression test and e) the true stress versus compression ratio of poly(dimethylsiloxane) (PDMS) bottlebrush elastomers, with a poly(acrylamide) (PAM) hydrogel. Reproduced with permission.^[24] Copyright 2016, Springer Nature. e) The tensile behavior of PDMS bottlebrush elastomers with a conventional elastomer with and without a prestrained structure, reproduced with permission.^[44]

2. Rheological Properties

2.1. Zero Shear Viscosity

Comb and bottlebrush polymer melts present a wide range of longest relaxation times, τ , plateau moduli, G_N^0 , and zero shear viscosities, $\eta_0 \approx \tau G_N^0$ relative to either their linear counterparts with the same total molecular weight or a linear polymer with a similar backbone length. Extensional properties of these combs and bottlebrushes, specifically their extensional viscosity, η_E , maximum polymer chain extensibility, λ^{max} , and strain hardening factor, $\text{SHF} \approx \eta_E^{\text{max}} / 3\eta_s$, strongly depend on their molecular characteristics. Tube (reptation) theory developed for comb polymers considers the effects of both entangled side chains and entangled backbone on the longest

relaxation time and plateau modulus of the polymer.^[22,38] For combs with entangled side chains, branching points are sluggish and therefore retard the reptation of backbone segments between the branching points until all of the side chains can relax. This means that side chains increase the longest relaxation time of the polymer via their strong frictional effect on the backbone. On the other hand, the tips of the arms (chain ends) in a molecule are highly mobile and relax faster than the other parts of the molecule via primitive path fluctuations (PPF) or contour length fluctuation (CLF) mechanisms. Increasing the chain ends (number of side chains, *q*) in a comb architecture accelerates this mechanism because the relaxed tips of the side chains dilute the tube of the backbone and reduce the longest relaxation time. Therefore, depending on the length and the number of entangled side chains, comb polymers have either

a longer or shorter relaxation time relative to their linear counterpart. Inkson et al.^[38] considered all of these mechanisms in the reptation theory and presented the following relation for the longest relaxation time of a comb polymer with entangled backbone and side chains

$$\tau_{\text{rep}} \propto Z_{\text{bb}}^2 \phi_{\text{bb}}^{2\alpha} q \tau_{\text{sc}} \quad (1)$$

where $1 < \alpha < 4/3$ is the dilution exponent, and ϕ_{bb} is the volume fraction of the backbone (see Figure 1). The exact value of dilution exponent α for branched polymers depends on the mathematical definition of relaxation mechanisms and moduli considered in the tube theory^[22,38,45,52,53] as well as the experimental method to define this value.^[54] It should be mentioned that Equation (1) considers combs with a limited number of side chains, $6 \leq q \leq Z_{\text{bb}}$. The upper limit of q in this model is equal to the number of entanglements of the backbone, Z_{bb} , where the branching point spacing is almost equal to one entanglement, $Z_{\text{g}} \approx 1$. The longest relaxation time of a side chain, τ_{sc} , is related to the innermost segments of the arms attached to the backbone, which exponentially depends on the length of the side chains

$$\tau_{\text{sc}} \propto \frac{\tau_e Z_{\text{sc}}^{3/2}}{(1 - \phi_{\text{sc}})^\alpha} \exp \left[\frac{15 Z_{\text{sc}} (1 - (1 - \phi_{\text{sc}})^{\alpha+1} (1 + (1 + \alpha) \phi_{\text{sc}}))}{4(1 + \alpha)(2 + \alpha) \phi_{\text{sc}}^2} \right] \quad (2)$$

where $\phi_{\text{sc}} = 1 - \phi_{\text{bb}}$ is the volume fraction of the side chains and τ_e is the Rouse relaxation time of one entanglement. Considering the relaxed side chains formally as a solvent for the backbone segments,^[45] the effective backbone modulus of a comb with entangled side chains reduces to $G_{\text{N},s}^0 = G_{\text{N}}^0 \phi_{\text{bb}}^{1+\alpha}$, where G_{N}^0 is the plateau modulus of the linear entangled polymer. The zero shear viscosity of a polymer melt can be approximately calculated from the product of the plateau modulus and the terminal relaxation time, $\eta_0 \approx \tau_{\text{rep}} G_{\text{N},s}^0$. For simplicity, α in Equations (1) and (2) was taken to equal 1, the volume fraction of side chains, ϕ_{sc} , was substituted with $1 - \phi_{\text{bb}}$, and $q Z_{\text{sc}}$ was replaced with $Z_{\text{bb}} (1 - \phi_{\text{bb}}) / \phi_{\text{bb}}$ to give

$$\eta_0 \propto \tau_e G_{\text{N}}^0 Z_{\text{bb}}^3 \phi_{\text{bb}}^2 (1 - \phi_{\text{bb}}) Z_{\text{sc}}^{1/2} \exp \left[\frac{5 Z_{\text{sc}} (1 + 2 \phi_{\text{bb}})}{8} \right] \quad (3)$$

It is worth mentioning that the right side of Equation (3) includes the term $\eta_{0,\text{bb}} \approx \tau_e G_{\text{N}}^0 Z_{\text{bb}}^3$ which is almost equal to the zero shear viscosity of the linear polymer (backbone in the absence of side chains). The middle part of Equation (3) contains a pure dilution term, $\phi_{\text{bb}}^2 (1 - \phi_{\text{bb}})$, which has the potential to reduce the η_0 of a comb below that of the linear backbone. However, the last term in Equation (3), $Z_{\text{sc}}^{1/2} \exp[5 Z_{\text{sc}} (1 + 2 \phi_{\text{bb}}) / 8]$, which is basically related to the strong frictional effect of the side chains on the backbone, increases the η_0 of a comb to a value that is not only above the zero shear viscosity of the linear backbone, $\eta_{0,\text{bb}} \approx \tau_e G_{\text{N}}^0 Z_{\text{bb}}^3$, but also, for long enough side arms, $Z_{\text{sc}} \gg 1$, raises η_0 above linear counterparts with the same total molecular weight. It should be mentioned that this friction term, $Z_{\text{sc}}^{1/2} \exp[5 Z_{\text{sc}} (1 + 2 \phi_{\text{bb}}) / 8]$, also contains a dilution term, $(1 + 2 \phi_{\text{bb}})$, which is related to the dynamic dilution effect of side chains on their own relaxation.^[52,53,55] Figure 3 shows the calculated zero shear viscosity of comb polyethylene (PE) versus the total molecular weight of the polymer, $M = M_{\text{bb}} + q M_{\text{bb}}$, using the same method presented in Equations (1)–(3) with a dilution exponent $\alpha = 4/3$, $\tau_e = 9.5 \times 10^{-9}$ s, and $M_e = 1150$ g mol⁻¹ for linear PE at 190 °C.^[38] The drawn power law line, $\eta_0 = 5.8 \times 10^{-14} M_w^{3.41}$ (with η_0 in Pa·s and M_w in g mol⁻¹) is the zero shear viscosity of linear reference PEs at 190 °C.^[56] Figure 3a was plotted for combs with $6 \leq Z_{\text{bb}} \leq 100$, $2 \leq Z_{\text{sc}} \leq 10$, and $6 \leq q \leq Z_{\text{bb}}$ as well as three-arm star PEs. It can be seen that there are upper and a lower boundaries for η_0 , which are related to three-arm stars and combs with a maximum number of branches, $q = Z_{\text{bb}}$, respectively. It can be concluded that the region above the linear reference encompasses the comb topologies whose side chains have a strong frictional effect on the backbone. In contrast, the region below the linear reference is composed of combs where the frictional effect of their side chains on η_0 is overcompensated by their strong dilution effect on the backbone, $\phi_{\text{bb}} \ll 1$.

Figure 3b shows that for certain backbone and side chain lengths, the zero shear viscosity follows an almost power-law function decrease with increasing number of side chains on the backbone, q , or total molecular weight (for instance, see the trend line for combs with $Z_{\text{bb}} = 100$ and $Z_{\text{sc}} = 10$). Our analysis

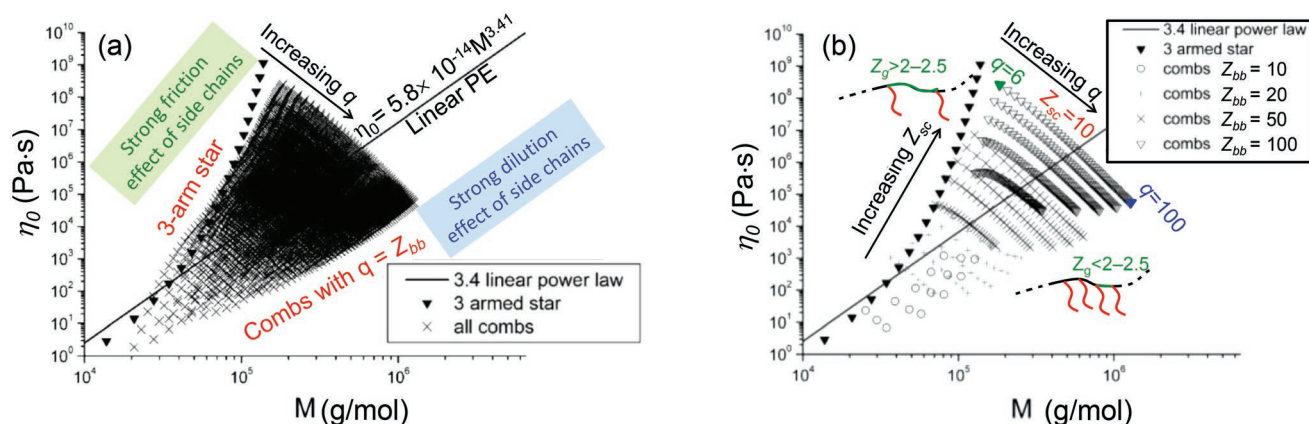


Figure 3. Zero shear viscosity of comb polyethylene as a function of total molecular weight for a) combs with different backbone lengths, $6 \leq Z_{\text{bb}} \leq 100$, side chain lengths, $2 \leq Z_{\text{sc}} \leq 10$, and number of side chains per backbone, $6 \leq q \leq Z_{\text{bb}}$, as well as the three-arm star polymers, and b) only four different series of combs with $Z_{\text{bb}} = 10, 20, 50,$ and 100 , where the length of side chains are $Z_{\text{sc}} = 2, 4, 6, 8,$ and 10 , and the number of side chains per backbone varied between the 6 and Z_{bb} . All panels reproduced with permission.^[38] Copyright 2006, American Chemical Society.

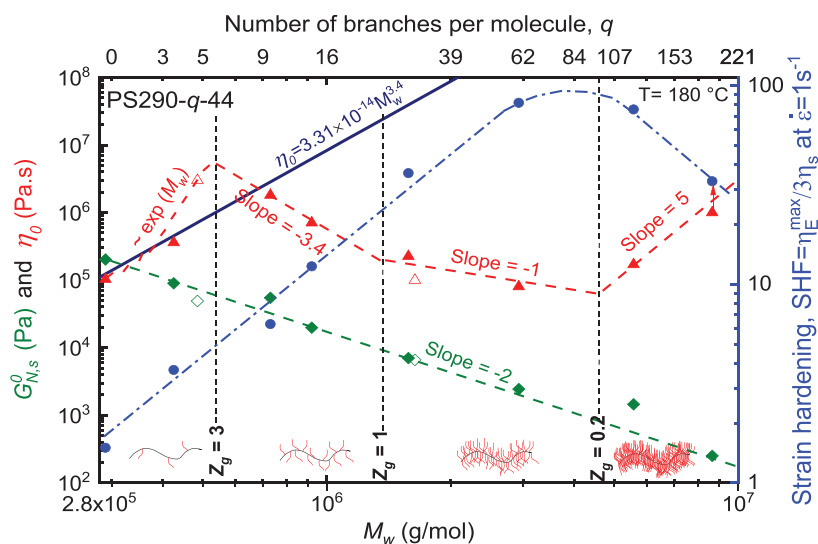


Figure 4. Zero shear viscosity, η_0 , diluted modulus, $G_{N,s}^0$, (right y-axis) and the strain hardening factor, SHF (left y-axis) as a function of the weight average molecular weight (bottom x-axis) and number of branches per molecule (top x-axis). Filled symbols are the samples from Abbasi et al.^[11] with $M_{w,bb} = 290 \text{ kg mol}^{-1}$, and open symbols are taken from Kempf et al.^[42] with $M_{w,bb} = 275 \text{ kg mol}^{-1}$. Dashed lines were drawn to guide the eye and the labeled scaling exponents are explained in the text. Reproduced with permission.^[11] Copyright 2017, American Chemical Society.

of η_0 of comb series with well-entangled backbone, $Z_{bb} > 20$, in Figure 3b shows that η_0 of combs with branching point spacing $Z_g > 2-2.5$ are above that of the linear reference, while η_0 of combs with $1 < Z_g < 2-2.5$ are below the linear counterparts. However, what is missing in Figure 3 is the zero shear viscosity of combs with higher number of side chains, i.e., $q > Z_{bb}$ or $Z_g < 1$. Experimental data for a series of nearly monodisperse comb polystyrenes (nomenclature: $PSM_{w,bb}-q-M_{w,sc}$) with similar backbone $M_{w,bb} = 290 \text{ kg mol}^{-1}$ ($Z_{bb} = 20$), and side chains $M_{w,sc} = 44 \text{ kg mol}^{-1}$ ($Z_{sc} = 3$), but a different number of branches per molecules, $0 < q < 190$, shown in Figure 4, demonstrate that η_0 increases exponentially with total molecular weight, $M_w = M_{w,bb} + qM_{w,sc}$, to a level that is even above their linear counterparts (solid line $\eta_0 = 3.31 \times 10^{-14} M_w^{3.4}$) for combs with $Z_g > Z_{sc}$. A relative maximum in η_0 seems to be related to a comb with approximately $Z_g = Z_{sc}$ (or equivalently a comb with $q = Z_{bb}/Z_{sc} - 1 \approx 6$ for this specific backbone and side chains). A further increase in q results in a reduction in the zero shear viscosity below the linear counterparts with an almost a power-law behavior, $\eta_0 \propto M_w^{-3.4}$, which is in agreement with the predictions shown in Figure 3b and Equation (3). The limited range of scaling laws for η_0 of these comb series (1–2 decades in η_0) is related to the limited number of entanglements in the backbone and side chains of these comb series, i.e., $Z_{bb} = 20$ and $Z_{sc} = 3$, respectively, which results in a limited range for the variation of longest relaxation times for this comb series. However, these scaling laws are in agreement with the predictions of reptation theory in Figure 3b and Equation (3) for the comb topologies with $q < Z_{bb}$. It should be mentioned that increase of Z_{bb} or Z_{sc} for such comb PS series might cause a very high η_0 above the linear counterparts for the loosely grafted combs, which might not be achieved easily within the

reasonable experimental temperature–frequency window, e.g., 130–240 °C for PS. Further reduction in η_0 as a function of M_w with increasing q was achieved for combs with $q > Z_{bb}$. In this highly branched region, the comb polymers have an unentangled branching point spacing, $Z_g < 1$, and η_0 reduces with a power of around 1 as a function of q . This means that the backbone of a comb-PS with an entangled branching point spacing, $1 < Z_g < Z_{sc}$, relaxes with a reptation mechanism, while the backbone of a comb with an unentangled branching point spacing relaxes with a Rouse mechanism. Figure 4 shows results for such a comb-PS series where a relative minimum in η_0 was observed for a comb-PS with $Z_g \approx 0.2$ which is almost equal to the η_0 of its linear polymer equivalent with the same backbone.^[11] Further increases in the number of branches on the same backbone to $q = 190$ significantly increased η_0 . Investigation of a series of densely grafted combs with longer backbone, $20 < Z_{bb}$, which most probably have lower η_0 than the linear counterpart, is needed for accurate analysis of these transitional regions toward the dense bottlebrush regime.

Abbasi et al.^[11] used the scaling analysis criteria of Sheiko and co-workers^[24,25] (see details in Section 3) for this series of grafted PS to classify them into comb and bottlebrush conformations. According to the length of the backbone and side chains (i.e., $Z_{bb} = 20$ and $Z_{sc} = 3$), grafted polymers with $142 < q < 951$, which is equivalent to $3 < n_g < 20$, have a loose bottlebrush topology and grafted polymers with lower values were classified as densely comb topology. Figure 4 shows that the plateau modulus almost reduces with the same scaling, $G_{N,s}^0 = G_{N,lin}^0 \phi_{bb}^2$, for the entire series of comb-PS. Now the question arises why the loose bottlebrush PS290-190-44 has a significantly higher η_0 than dense comb PS290-120-44 even though its diluted modulus is lower. This behavior might be related to difference between the frictional coefficient of comb and bottlebrushes. In comb polymers, the frictional effect of side chains exponentially increases with the length of side chains (see Equations (2) and (3)). While López-Barrón et al.^[18,19] showed that in a series of densely grafted bottlebrushes with short side chains ($n_{sc} \leq 16$), the monomeric friction coefficient, ξ , decreases upon increasing the side chain length, due to the lower flexibility combined with the higher distance (free volume) between adjacent bottlebrush backbones and consequently lower glass transition temperature, T_g . Transition from the dense comb to loose bottlebrush regimes (see Section 3) results in a complex behavior where the ends of the entangled side chains of loose bottlebrush topologies might be able to penetrate between the side chains of neighboring molecules during deformation. Due to the very tight spacing between the branching points, the diffusion coefficient ($D = kT/\xi$, where ξ is the total friction coefficient of side chains) of the trapped part of the side chains significantly decreases, which results in longer arm relaxation times. This transition in rheological behaviors depends on

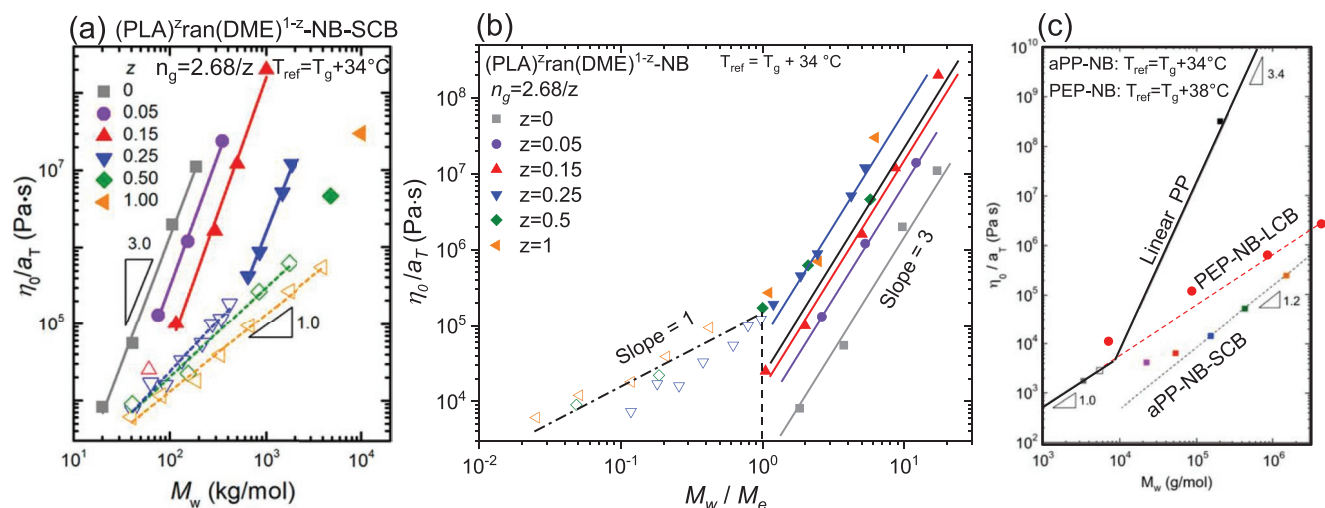


Figure 5. a) Reduced zero shear viscosity versus weight-average molecular weight, M_w for bottlebrushes with a fixed length of short chain branches (SCB) of polylactide (PLA, $M_n = 3.5 \text{ kg mol}^{-1}$, $M_n/M_{e,PLA} \approx 0.4$) synthesized by ROMP of ω -norbornenyl polylactide macromonomers and norbornene dimethyl ester (DME) as comonomer to vary the grafting densities, $^{[59]}$ $z \equiv 2.68/n_g$, $\text{PLA}^2\text{-ran(DME)}^{1-z}\text{-NB-SCB}$. The backbone degree of polymerization was varied in these series. Reproduced with permission. $^{[31]}$ Copyright 2018, American Chemical Society. b) Reduced zero shear viscosity versus number of entanglements on the bottlebrush strand, $M_{e,s} = \rho RT/G_{N,s}^0$ for bottlebrushes in (a). Reproduced with permission. $^{[31]}$ Copyright 2018, American Chemical Society. c) Reduced zero shear viscosity versus M_w of two bottlebrush series with $n_g = 1$: aPP-NB-SCB with short chain branches of atactic polypropylene (aPP, $M_n = 2.05 \text{ kg mol}^{-1}$, $M_n/M_{e,aPP} \approx 0.5$), $^{[29]}$ and PEP-NB-LCB with long chain branches (LCB) of entangled poly-ethylene-alt-propylene (PEP, $M_n = 6.7 \text{ kg mol}^{-1}$, $M_n/M_{e,PEP} \approx 3.5$) $^{[30]}$ The line with a slope of 3.4 is for the linear reference PP. Reproduced with permission. $^{[29,30]}$ Copyright 2014 and 2015, American Chemical Society.

grafting density and most probably the DP of side chains. However, to the best of our knowledge, this behavior has not been systematically studied yet.

Several studies investigated the zero shear viscosity η_0 as a function of total molecular weight for different series of loose and dense bottlebrushes with either short chain branches (SCB) $^{[13,18,19,24,29-31,57]}$ or long chain branches (LCB). $^{[11,30]}$ Within these bottlebrush series, two characteristics out of n_{sc} , n_g , and n_{bb} are fixed and one of them is varied in the series. **Figure 5a** presents the reduced η_0 for five bottlebrush series and a linear series at a reference temperature $T_{ref} = T_g + 34 \text{ }^\circ\text{C}$. All of the bottlebrush series are poly-(norbornene)-graft-poly(\pm -lactide) with a fixed length of SCB polylactide (PLA, $M_n = 3.5 \text{ kg mol}^{-1}$, $M_n/M_{e,PLA} \approx 0.4$). These bottlebrushes were synthesized via ROMP of ω -norbornenyl polylactide macromonomers. Norbornene dimethyl ester (DME) as comonomer was used to vary the grafting density in the range of $0 < z < 1$, where $n_g = 2.68/z$. Each series has a fixed grafting density and n_{sc} , but the degree of polymerization of the backbone, n_{bb} , was varied. $^{[31]}$ It was shown that η_0 versus M_w has two different scaling regimes 1 and 3, which could be related to Rouse and reptation dynamics, respectively. This demonstrates that grafting density strongly impacts the apparent entanglement molar mass of bottlebrushes. **Figure 5b** shows these data as a function of the number of entanglements in the bottlebrush strands. The entanglement molecular weight, M_e , of these bottlebrushes was calculated from the diluted modulus, $M_e = \rho RT/G_{N,s}^0$, which was defined from the van Gurp-Palmen plots as the value of $[G^*]$ or G' at the minimum value of $\tan(\delta)$ within the entanglement regime. $^{[58]}$ It can be seen in **Figure 5b** that the Rouse and reptation relaxation mechanisms have a sharp transition at $M_w/M_e = 1$. This means that in principle similar to linear polymers, the number

of entanglements in the bottlebrush strands with SCB structure plays the most important role in the increase of η_0 for bottlebrushes. The main difference between the linear and SCB-bottlebrushes is related to the friction coefficient, where in the linear polymers is due to the monomers on the backbone but in SCB-bottlebrushes is caused by monomers on the surface of the bottlebrush cylinders. It is also clear that vertical shift of the η_0 data in entangled region in **Figure 5b** is related to the increase in the diluted modulus of densely grafted bottlebrushes with branching point spacing, $^{[24]}$ $G_{N,DB}^0 \propto (n_g/n_{sc})^{3/2}$.

Grubbs and co-workers $^{[13]}$ showed that the scaling exponent of the zero shear viscosity–molecular weight dependence of a series of entangled wedge polymers (very dense bottlebrushes with three branches per repeating unit of backbone, i.e., $n_g \approx 0.3$) with SCB structure might be even above the 3 power law with an exponent of around 4.2. However, there were only four samples available for this series.

The zero shear viscosity for two series of bottlebrushes with $n_g = 1$ are shown in **Figure 5c**. The first series, aPP-NB-SCB, had short chain branches that were unentangled side chains of atactic polypropylene (aPP, $M_n = 2.05 \text{ kg mol}^{-1}$, $M_n/M_{e,aPP} \approx 0.5$), $^{[29]}$ while the second series, PEP-NB-LCB, had long chain branches of entangled side chains of poly-ethylene-alt-propylene (PEP, $M_n = 6.7 \text{ kg mol}^{-1}$, $M_n/M_{e,PEP} \approx 3.5$), $^{[30]}$ both prepared from norbornenyl-terminated macromonomers. In both series, the DP of the backbone was below the entanglement length, $n_{bb} < n_{e,bb}$, and both series show almost a Rouse relaxation mechanism for η_0 . This means that for densely grafted bottlebrushes, $n_g = 1$, even side chains long enough to have originally 3.5 entanglements are fully stretched and cannot penetrate into neighboring side chains or flexible bottlebrush cylinders to respond like an entangled system.

It can be concluded that η_0 of the bottlebrushes strongly depends on the number of entanglements in the bottlebrush filament as well as the DP of the side chains (Figure 5); however, the dependency of η_0 for loose bottlebrush systems with entangled side chains on the DP of the side chains is stronger due to penetration of side chains into neighboring molecules, which results in entangled systems (Figure 4).

2.2. Strain Hardening Factor

The preceding analyses in Figure 4 revealed that the number of branches in a comb polymer with a given backbone and side chain length can be optimized to achieve a minimum in the shear viscosity, which is important for the processability of polymers under shear deformations. However, optimization of the molecular structure of branched polymers for extensional processes, e.g., film blowing, should take into account both shear and extensional behaviors and especially the strain hardening property. The original pom-pom model for sufficiently high extensional rates predicts the strain hardening factor to be^[60]

$$\text{SHF} = \eta_E^{\text{max}} / 3\eta_s \approx \lambda_{\text{max}}^2 \tau_s / \tau_b \quad (4)$$

where $\tau_s = qZ_{\text{bb}}\tau_{\text{sc}}$ and $\tau_b = 4/\pi^2 qZ_{\text{bb}}^2 \phi_{\text{bb}} \tau_{\text{sc}}$ are the stretch and orientation relaxation times of the backbone, respectively, and the maximum limiting stretch of the backbone, λ_{max} , is equal to q when there are q dangling arms on each side for a total of $2q$ side chains per molecule, $\lambda_{\text{max}} = q$. Equation (4) can be simplified to $\text{SHF} = q^2 Z_{\text{bb}}^{-1} \phi_{\text{bb}}^{-1}$, which shows that for a given backbone and side chain length, SHF scales with q^3 or M^3 . This scaling is a bit stronger than the experimentally observed scaling for SHF at $\dot{\epsilon} = 1\text{s}^{-1}$ for the comb series shown in Figure 4 (right γ -axis), which was $\text{SHF} \propto q^{1.7} \propto M^{1.7}$. The concept of a constitutive equation for the pom-pom model was extended for more complicated branched topologies, e.g., Cayley trees,^[61] randomly branched polymers,^[62,63] as well as comb structures.^[64] For comb polymers with multiple branching points, equivalent to a pom-pom molecule with $2q$, the maximum limiting stretch of the backbone segments hierarchically increases from 1 for the outermost segments of the backbone to almost q for the innermost ones located in the middle of the backbone. Therefore, the average maximum stretching of a backbone within a comb should be lower than that of a pom-pom with the same amount of branches. Liu et al.^[12] showed that a comb PS with well-entangled branching point spacing ($Z_s \approx 10$) has a maximum in the engineering stress that emerges at a stretching ratio of $\lambda_{\text{max}} \approx 4\sqrt{Z_{\text{bb}}}$ rather than $\lambda_{\text{max}} = q$ for the pom-pom model. Consequently, the strain hardening for comb polymers in Equation (4) is a weaker function of the number of branches (or molecular weight for a certain backbone), $\text{SHF} \propto \phi_{\text{bb}}^{-1} \propto M \propto q$, than the original pom-pom equation, $\text{SHF} = q^2 Z_{\text{bb}}^{-1} \phi_{\text{bb}}^{-1} \propto M^3 \propto q^3$. Figure 4 shows that the SHF levels off or even decreases with further increase in q or decrease in Z_g for this series of combs with similar backbone and side chains. This means that stretchability of segments between the branch points reduces as soon as the conformation of backbone shift to a loose bottlebrush conformation with inherently stretched segments. The maximum SHF almost matches the minimum observed for η_0

in this comb series, where a transition from the comb to bottlebrush regimes occurred, $Z_g \approx 0.2$. From a processing point of view, a polymer with minimum shear viscosity and a maximum in SHF is an ideal structure for extensional process, e.g., film blowing and foaming. We showed that these properties in a comb structure can be achieved through an optimum number of branches or branching point spacing. The branching point spacing $Z_g \approx 0.2$ might not be a universal number for other backbones; however, it seems that Z_g should be at least smaller than 1 to achieve the minimum in η_0 . In order to find a more accurate and universal equation, a detailed scaling analysis for relaxation time and plateau modulus, especially for the transition from comb to bottlebrush, is needed to define a general equation for this proposed optimum number of branches. In the next section, this analysis was done for plateau modulus.

3. Diluted Plateau Shear Modulus

Entangled linear polymer melts typically possess a plateau modulus $G_N^0 \approx 10^5 - 10^6$ Pa that is consistent with their entanglement molecular weights, $M_e = \rho RT / G_N^0 \approx 10^3 - 10^4$ g mol⁻¹. The presence of low molecular weight components (e.g., solvents or oligomers) in a melt of entangled polymers increases $M_{e,s}$ as $M_{e,s} \approx M_e \phi^{-\alpha}$ and consequently decreases the plateau modulus of the concentrated entangled system, $G_{N,s}^0 \approx G_N^0 \phi^{1+\alpha}$ with $1 < \alpha < 4/3$.^[65] The side chains of comb and bottlebrush polymers, which relax faster than their backbones, dilute the tube diameter of the backbone and consequently also behave like a solvent. Fetters et al.^[36,66] obtained two empirical relationships for the plateau modulus of poly(α -olefins)

$$G_N^0 = 24820 m_b^{-3.49} \quad m_b = 14 - 28 \text{ g mol}^{-1} \quad (5a)$$

$$G_N^0 = 41.84 m_b^{-1.58} \quad m_b = 35 - 56 \text{ g mol}^{-1} \quad (5b)$$

where G_N^0 is given in MPa, m_b is the average molecular weight per backbone bond and, analogous to bottlebrush structures, is proportional to the inverse of the volume fraction of the backbone bonds, ϕ_{bb}^{-1} . López-Barrón et al.^[18] reported the rheological data of a series of ultrahigh molecular weight poly(α -olefins) with bottlebrush architectures, ranging from poly(1-hexene) to poly(1-octadecene). The rubbery plateau modulus was clearly achieved

$$G_N^0 = 1.05 n_{\text{sc}}^{-1.47} = 1.05 \left(\frac{1}{7} m_b - 2 \right)^{-1.47} \quad m_b = 42 - 126 \text{ g mol}^{-1} \quad (5c)$$

where $m_b = 14 + 7n_{\text{sc}}$. These empirical equations, Equations (5a)–(5c), are consistent with the scaling analysis of Sheiko and co-workers for bottlebrush polymers with rod-like side chains.^[32] Sheiko and co-workers^[16,24,25] investigated the effect of side chain spacing on the conformations of the backbone and side chains as well as the plateau modulus for comb and bottlebrush polymers. It was shown that the molecular conformation of a comb topology in the melt phase depends on the DP of the side chains, n_{sc} , and DP of the backbone spacer between grafting points, n_g .^[25,44] Using a scaling analysis, they distinguished between four different conformational regimes:

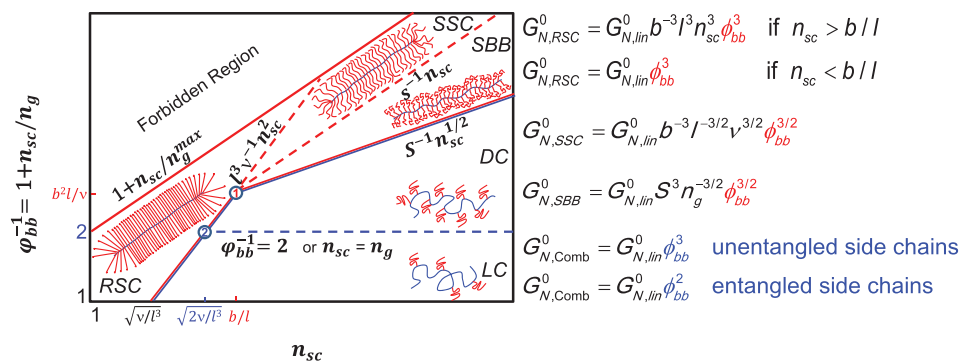


Figure 6. Different conformational regimes of comb and bottlebrushes in the framework of ϕ_{bb}^{-1} versus n_{sc} . The two relevant dimensionless parameters are $s = v/(bl^2)$ and $S = v/(bl)^{3/2}$, where v is the monomeric volume, l is the monomeric length, and b is the Kuhn length of the polymer. Equations on the right side are for the corresponding moduli of these regions. The equations are from^[8] and the graph is reproduced with permission.^[16] Copyright 2018, American Chemical Society.

loosely grafted comb (LC), densely grafted comb (DC), loosely grafted bottlebrush (LB), and densely grafted bottlebrush (DB), according to the n_{sc} and n_g of the polymers. In their recent work,^[32] they divided the bottlebrush regime into three different subregions including stretched backbone (SBB), stretched side chain (SSC), and rod-like side chain (RSC) according to the volume fraction of the backbone, $\phi_{bb} = n_g/(n_g + n_{sc})$ and n_{sc} . However, the LB and DB regions are basically consistent with the SBB and SSC regimes, respectively, and the RSC region describes a class of bottlebrushes with very short side chain lengths. **Figure 6** shows these conformational regimes in the framework of ϕ_{bb}^{-1} versus n_{sc} for these systems. In the right side of **Figure 6**, the corresponding equations for the moduli of these regions are shown.

Both the backbone and side chains in LC and DC polymers have almost unperturbed random Gaussian conformations; however, DC polymers have shorter side chains than the branching point spacer, $n_s < n_g$. The total number of monomers between the entanglements, n_e , as well as the plateau modulus of entangled comb and bottlebrush systems, $G_N^0 = kT/V_e$, were defined based on the Kavassalis–Noolandi conjecture,^[67] which states that there is an almost fixed, $P_e \cong 20.8 \pm 0.8$, number of sections of different chains within the volume of an entanglement strand, $V_e = vn_e$, (v is monomeric volume).

This concept results in a relation for the modulus $G_{N,Comb}^0 = G_{N,lin}^0 \phi_{bb}^3$ for both LC and DC polymers,^[24,25] where $G_{N,lin}^0$ is the plateau modulus of an entangled linear polymer. However, this scaling is different compared to previous findings for comb polymers with entangled side chains. Further reduction in the branching point spacing, n_g , at constant n_s (or increasing $\phi_{bb}^{-1} = n_{sc}/n_g + 1$) toward SBB bottlebrush structures results in the segregation of molecules and reduces the overlap of side chains belonging to neighboring bottlebrushes. The backbone in an SBB is stretched due to side chain crowding, while the side chains still maintain their unperturbed conformations. In this regime the rubber plateau modulus, $G_{N,SBB}^0 = G_{N,lin}^0 S^3 n_g^{-3/2} \phi_{bb}^{3/2}$, depends on the length of the side chains (i.e., $G_{N,SBB}^0 \propto n_g^{-3/2} \phi_{bb}^{3/2} \approx n_{sc}^{-3/2}$), where $S = v/(bl)^{3/2}$ is a dimensionless number, v is the monomeric volume, l is the monomeric length, and b is the Kuhn length of the polymer. Further reduction in n_g at constant n_s (or increasing of ϕ_{bb}^{-1})

results in an SSC molecule, where both the backbone and side chains adopt stretched conformations. This means that the side chains of an SSC molecule theoretically cannot interpenetrate the side chains of neighboring molecules. In the SSC regime, the rubber plateau modulus, $G_{N,SSC}^0 = G_{N,lin}^0 b^{-3} l^{-3/2} v^{3/2} \phi_{bb}^{3/2}$, scales with $\phi_{bb}^{3/2}$, however n_g is very close to 1 and no longer has a strong effect on the modulus. It is interesting to note that, for both SSC and SBB regimes, the rubber plateau modulus has a similar scaling as Equation (5b) for poly(α -olefins) with $m_b = 35 - 56 \text{ g mol}^{-1}$. In other words, dense bottlebrush topologies behave like poly(α -olefins) with $m_b = 35 - 56 \text{ g mol}^{-1}$. **Figure 6** shows another regime for bottlebrushes with fully stretched side chains and backbone, called the RSC regime. The side chains in the RSC regime are below a certain limit so that $b^{-3} l^3 v n_{sc}^2 < \phi_{bb}^{-1}$. The modulus in this regime scales with $G_{N,RSC}^0 \propto \phi_{bb}^{3/2}$ which is also similar to the scaling for poly(α -olefins) with $m_b = 14 - 28 \text{ g mol}^{-1}$ shown in Equation (5a).

It should be mentioned that the scaling analysis for all three regimes of bottlebrushes, SBB, SSC, and RSC, was only investigated experimentally for bottlebrushes with unentangled side chains. Dalsin et al.^[30] investigated the modulus and rheological properties of a series of bottlebrushes with entangled side chains; however, the whole bottlebrush strand was not entangled, and still acted as a Rouse molecule. Increasing the length of side chains of a bottlebrush to above a certain limit (e.g., longer than one entanglement) might facilitate the penetration of side chains into neighboring molecules as the side chain ends might be located outside the backbone tube.

One of the breakthrough applications of bottlebrushes with a substantially lower plateau modulus is bottlebrush elastomers with a permanent network structure. These elastomers have intrinsic supersoft and superelastic properties without additional solvents and are promising candidates for synthetic substitutes of biological tissues.^[68] Therefore, another important parameter affecting the network shear modulus is the crosslink density,^[7,24,33,34,69] or the DP of the bottlebrush backbone between crosslinks, n_x .^[34,69] It was shown that for dense bottlebrush networks with $n_g = 1$ and fully stretched strands between crosslinks ($\approx n_x b$) that were longer than the bottlebrush Kuhn length, $b_k = v^{1/2} l^{-1/2} n_{sc}^{1/2} \approx n_{sc}^{1/2}$, i.e., $n_x b \gg n_{sc}^{1/2}$, the

bottlebrush network behaved in a similar way to a flexible filament with a network shear modulus given by^[16,46]

$$G_{\text{BB}}^0 \approx \rho k T n_x^{-1} (n_{\text{sc}} + 1)^{-1} \quad (6)$$

Equation (6) shows that the modulus of such a bottlebrush elastomer is, by a factor of $(n_{\text{sc}} + 1)^{-1}$, smaller than that of conventional elastomers. In other words, the modulus of these bottlebrushes can simply be adjusted by the DP of the side chains. However, bottlebrushes with strands shorter than the bottlebrush Kuhn length behave as semiflexible filaments with a weaker dependence of the shear modulus on the side chain length, $G_{\text{BB}}^0 \propto n_{\text{sc}}^{-0.5}$.

4. Conclusions and Outlook

This paper discussed the effect of the molecular structure of combs and bottlebrushes on the most important rheological and mechanical properties in both shear and elongation. Comb topologies with entangled side chains are interesting due to their pronounced strain hardening behavior under extensional flows. The SHF increases with an increase in the number of side chains for a given backbone and levels off when the minimum zero shear viscosity, η_0 , was reached. The origin of strain hardening in comb polymers is the stretchability of branching point spacing in a diluted environment. This means that an enough flexible backbone diluted with enough side chains results in a maximum SHF and minimum zero shear viscosity. The transition from a dense comb to a loose bottlebrush topology for entangled systems drastically increases η_0 and reduces SHF for a given backbone and side chain length. The origin of this transition for η_0 could be related to the different monomeric frictions in comb and bottlebrush structures. Penetration of entangled side chains of comb topologies into neighboring molecules results in higher frictional coefficient for combs with longer side chains, while intermolecular penetration is diminished for dense bottlebrush topologies which results in lower frictional effect in bottlebrushes with longer side chains. However, this phenomenon should be quantified using scaling analysis of relaxation times. This means that the frictional mechanisms for dense comb and loose bottlebrushes should be revisited according to the penetration of side chains of neighboring molecules. For a better understanding of these frictional coefficients, the extensional experiments should be performed. To the best of our knowledge, there are wide range of experimental data for linear rheological behavior of densely grafted comb and loosely grafted bottlebrushes; however, the lack of both uniaxial and biaxial extensional properties of such systems is obvious. Performing these extensional experiments in the melt state might help to quantify and understand the frictional mechanisms in transitional region from comb to bottlebrush topology. The plateau modulus of both comb and bottlebrushes were investigated based on the scaling analysis. Different conformations of backbone and side chains in comb and bottlebrushes were investigated according to the degree of polymerization of the side chains, n_{sc} , branching point spacing, n_{g} , and the volume fraction of the backbone, ϕ_{bb} . The shear plateau modulus of all conformational regimes was presented and

correlated to n_{sc} , n_{g} , and ϕ_{bb} , as well as to the average monomeric volume and length. The volume fraction of the backbone, as well as the length of the side chains in dense bottlebrush topologies, plays the most important roles in the resulting rubber plateau shear modulus of the bottlebrush melts. Bottlebrush elastomers (networks) present solvent-free, super-soft, and superelastic behavior via a controlled network shear modulus through the length of the side chains and crosslink density.

Acknowledgements

M.A. gratefully acknowledges the Alexander von Humboldt Foundation and the German Science Foundation, DFGWI1911/18-2, for financial support. The authors thank Prof. Sergei Sheiko and Prof. Frank Bates for fruitful discussion and Dr. Jennifer Kübel for proofreading of this article. The authors also thank the reviewers of this manuscript for several excellent suggestions.

Conflict of Interest

The authors declare no conflict of interest.

Keywords

bottlebrush, comb, extensional rheology, linear rheology, strain hardening, zero shear viscosity

Received: October 7, 2018
Revised: December 16, 2018
Published online: February 21, 2019

- [1] J. Roovers, *Polymer* **1979**, *20*, 843.
- [2] M. Wintermantel, M. Gerle, K. Fischer, M. Schmidt, I. Wataoka, H. Urakawa, K. Kajiwara, Y. Tsukahara, *Macromolecules* **1996**, *29*, 978.
- [3] S. S. Sheiko, B. S. Sumerlin, K. Matyjaszewski, *Prog. Polym. Sci.* **2008**, *33*, 759.
- [4] J. Li, M. Gauthier, *Macromolecules* **2001**, *34*, 8918.
- [5] D. Pantazis, I. Chalari, N. Hadjichristidis, *Macromolecules* **2003**, *36*, 3783.
- [6] Y. Xia, J. A. Kornfield, R. H. Grubbs, *Macromolecules* **2009**, *42*, 3761.
- [7] K. Matyjaszewski, *Adv. Mater.* **2018**, *30*, 1706441.
- [8] K. Huang, J. Rzyayev, *J. Am. Chem. Soc.* **2009**, *131*, 6880.
- [9] R. Verduzco, X. Li, S. L. Pesek, G. E. Stein, *Chem. Soc. Rev.* **2015**, *44*, 2405.
- [10] J. Roovers, W. W. Graessley, *Macromolecules* **1981**, *14*, 766.
- [11] M. Abbasi, L. Faust, K. Riazi, M. Wilhelm, *Macromolecules* **2017**, *50*, 5964.
- [12] G. Liu, H. Ma, H. Lee, H. Xu, S. Cheng, H. Sun, T. Chang, R. P. Quirk, S.-Q. Wang, *Polymer* **2013**, *54*, 6608.
- [13] M. Hu, Y. Xia, C. S. Daefler, J. Wang, G. B. McKenna, J. A. Kornfield, R. H. Grubbs, *J. Polym. Sci., Part B: Polym. Phys.* **2015**, *53*, 899.
- [14] T.-P. Lin, A. B. Chang, H.-Y. Chen, A. L. Liberman-Martin, C. M. Bates, M. J. Voegtle, C. A. Bauer, R. H. Grubbs, *J. Am. Chem. Soc.* **2017**, *139*, 3896.
- [15] A. B. Chang, T.-P. Lin, N. B. Thompson, S.-X. Luo, A. L. Liberman-Martin, H.-Y. Chen, B. Lee, R. H. Grubbs, *J. Am. Chem. Soc.* **2017**, *139*, 17683.

- [16] H. Liang, B. J. Morgan, G. Xie, M. R. Martinez, E. B. Zhulina, K. Matyjaszewski, S. S. Sheiko, A. V. Dobrynin, *Macromolecules* **2018**, *51*, 10028.
- [17] C. R. López-Barrón, A. H. Tsou, J. M. Younker, A. I. Norman, J. J. Schaefer, J. R. Hagadorn, J. A. Throckmorton, *Macromolecules* **2018**, *51*, 872.
- [18] C. R. López-Barrón, A. H. Tsou, J. R. Hagadorn, J. A. Throckmorton, *Macromolecules* **2018**, *51*, 6958.
- [19] C. R. López-Barrón, P. Brant, A. P. R. Eberle, D. J. Crowther, *J. Rheol.* **2015**, *59*, 865.
- [20] Y. Tsukahara, S.-I. Namba, J. Iwasa, Y. Nakano, K. Kaeriyama, M. Takahashi, *Macromolecules* **2001**, *34*, 2624.
- [21] K. Kunal, C. G. Robertson, S. Pawlus, S. F. Hahn, A. P. Sokolov, *Macromolecules* **2008**, *41*, 7232.
- [22] D. R. Daniels, T. C. B. McLeish, B. J. Crosby, R. N. Young, C. M. Fernyhough, *Macromolecules* **2001**, *34*, 7025.
- [23] M. Rubinstein, R. H. Colby, *Polymer Physics*, Vol. 23, Oxford University Press, New York **2003**.
- [24] W. F. M. Daniel, J. Burdynska, M. Vatankhah-Varnoosfaderani, K. Matyjaszewski, J. Paturej, M. Rubinstein, A. V. Dobrynin, S. S. Sheiko, *Nat. Mater.* **2016**, *15*, 183.
- [25] J. Paturej, S. S. Sheiko, S. Panyukov, M. Rubinstein, *Sci. Adv.* **2016**, *2*, e1601478.
- [26] M. W. Kyu Hyun, C. O. Klein, K. S. Cho, J. G. Nam, K. H. Ahn, S. J. Lee, R. H. Ewoldt, G. H. McKinley, *Prog. Polym. Sci.* **2011**, *36*, 1697.
- [27] M. A. Cziep, M. Abbasi, M. Heck, L. Arens, M. Wilhelm, *Macromolecules* **2016**, *49*, 3566.
- [28] K. Riazi, J. Kübel, M. Abbasi, K. Bachtin, S. Indris, H. Ehrenberg, R. Kádár, M. Wilhelm, *Polymer* **2016**, *104*, 240.
- [29] S. J. Dalsin, M. A. Hillmyer, F. S. Bates, *ACS Macro Lett.* **2014**, *3*, 423.
- [30] S. J. Dalsin, M. A. Hillmyer, F. S. Bates, *Macromolecules* **2015**, *48*, 4680.
- [31] I. N. Haugan, M. J. Maher, A. B. Chang, T.-P. Lin, R. H. Grubbs, M. A. Hillmyer, F. S. Bates, *ACS Macro Lett.* **2018**, *7*, 525.
- [32] H. Liang, Z. Cao, Z. Wang, S. S. Sheiko, A. V. Dobrynin, *Macromolecules* **2017**, *50*, 3430.
- [33] H. Liang, S. S. Sheiko, A. V. Dobrynin, *Macromolecules* **2018**, *51*, 638.
- [34] Z. Cao, W. F. M. Daniel, M. Vatankhah-Varnoosfaderani, S. S. Sheiko, A. V. Dobrynin, *Macromolecules* **2016**, *49*, 8009.
- [35] S. Wijesinghe, D. Perahia, G. S. Grest, *Macromolecules* **2018**, *51*, 7621.
- [36] D. J. Lohse, S. T. Milner, L. J. Fetters, M. Xenidou, N. Hadjichristidis, R. A. Mendelson, C. A. García-Franco, M. K. Lyon, *Macromolecules* **2002**, *35*, 3066.
- [37] M. Kapnistos, D. Vlassopoulos, J. Roovers, L. G. Leal, *Macromolecules* **2005**, *38*, 7852.
- [38] N. J. Inkson, R. S. Graham, T. C. B. McLeish, D. J. Groves, C. M. Fernyhough, *Macromolecules* **2006**, *39*, 4217.
- [39] J. K. Nielsen, H. K. Rasmussen, M. Denberg, K. Almdal, O. Hassager, *Macromolecules* **2006**, *39*, 8844.
- [40] M. Kapnistos, K. M. Kirkwood, J. Ramirez, D. Vlassopoulos, L. G. Leal, *J. Rheol.* **2009**, *53*, 1133.
- [41] M. Kempf, V. C. Barroso, M. Wilhelm, *Macromol. Rapid Commun.* **2010**, *31*, 2140.
- [42] M. Kempf, D. Ahirwal, M. Cziep, M. Wilhelm, *Macromolecules* **2013**, *46*, 4978.
- [43] H. Lentzakis, D. Vlassopoulos, D. J. Read, H. Lee, T. Chang, P. Driva, N. Hadjichristidis, *J. Rheol.* **2013**, *57*, 605.
- [44] M. Vatankhah-Varnoosfaderani, W. F. M. Daniel, A. P. Zhushma, Q. Li, B. J. Morgan, K. Matyjaszewski, D. P. Armstrong, R. J. Spontak, A. V. Dobrynin, S. S. Sheiko, *Adv. Mater.* **2017**, *29*, 1604209.
- [45] S. T. Milner, T. C. B. McLeish, *Macromolecules* **1997**, *30*, 2159.
- [46] D. Neugebauer, Y. Zhang, T. Pakula, S. S. Sheiko, K. Matyjaszewski, *Macromolecules* **2003**, *36*, 6746.
- [47] T. Pakula, Y. Zhang, K. Matyjaszewski, H.-I. Lee, H. Boerner, S. Qin, G. C. Berry, *Polymer* **2006**, *47*, 7198.
- [48] L.-H. Cai, T. E. Kodger, R. E. Guerra, A. F. Pegoraro, M. Rubinstein, D. A. Weitz, *Adv. Mater.* **2015**, *27*, 5132.
- [49] F. Stadler, A. Nishioka, J. Stange, K. Koyama, H. Münstedt, *Rheol. Acta* **2007**, *46*, 1003.
- [50] M. H. Wagner, H. Bastian, P. Hachmann, J. Meissner, S. Kurzbeck, H. Münstedt, F. Langouche, *Rheol. Acta* **2000**, *39*, 97.
- [51] G. Xie, M. R. Martinez, M. Olszewski, S. S. Sheiko, K. Matyjaszewski, *Biomacromolecules* **2019**, *20*, 27.
- [52] J. M. Dealy, D. J. Read, R. G. Larson, in *Structure and Rheology of Molten Polymers*, Carl Hanser Verlag GmbH & Co. KG, Germany **2018**, p. 307.
- [53] S. T. Milner, T. C. B. McLeish, R. N. Young, A. Hakiki, J. M. Johnson, *Macromolecules* **1998**, *31*, 9345.
- [54] T. Shahid, Q. Huang, F. Oosterlinck, C. Clasen, E. van Ruymbeke, *Soft Matter* **2017**, *13*, 269.
- [55] R. C. Ball, T. C. B. McLeish, *Macromolecules* **1989**, *22*, 1911.
- [56] J. Janzen, R. H. Colby, *J. Mol. Struct.* **1999**, *485–486*, 569.
- [57] M. Hu, Y. Xia, G. B. McKenna, J. A. Kornfield, R. H. Grubbs, *Macromolecules* **2011**, *44*, 6935.
- [58] Z. Qian, G. B. McKenna, *Polymer* **2018**, *155*, 208.
- [59] I. N. Haugan, M. J. Maher, A. B. Chang, T.-P. Lin, R. H. Grubbs, M. A. Hillmyer, F. S. Bates, *ACS Macro Lett.* **2018**, *7*, 1039.
- [60] T. C. B. McLeish, R. G. Larson, *J. Rheol.* **1998**, *42*, 81.
- [61] E. van Ruymbeke, E. B. Muliawan, S. G. Hatzikiriakos, T. Watanabe, A. Hirao, D. Vlassopoulos, *J. Rheol.* **2010**, *54*, 643.
- [62] D. A. Daniel, J. Read, C. Das, J. den Doelder, M. Kapnistos, I. Vittorias, T. C. B. McLeish, *Science* **2011**, *333*, 1871.
- [63] C. Das, D. J. Read, D. Auhl, M. Kapnistos, J. den Doelder, I. Vittorias, T. C. B. McLeish, *J. Rheol.* **2014**, *58*, 737.
- [64] H. Lentzakis, C. Das, D. Vlassopoulos, D. J. Read, *J. Rheol.* **2014**, *58*, 1855.
- [65] M. Doi, *The Theory of Polymer Dynamics*, Oxford University Press, Great Britain **1986**.
- [66] L. J. Fetters, D. J. Lohse, C. A. García-Franco, P. Brant, D. Richter, *Macromolecules* **2002**, *35*, 10096.
- [67] T. A. Kavassalis, J. Noolandi, *Macromolecules* **1989**, *22*, 2709.
- [68] M. Vatankhah-Varnoosfaderani, A. N. Keith, Y. Cong, H. Liang, M. Rosenthal, M. Sztucki, C. Clair, S. Magonov, D. A. Ivanov, A. V. Dobrynin, S. S. Sheiko, *Science* **2018**, *359*, 1509.
- [69] Z. Cao, J.-M. Y. Carrillo, S. S. Sheiko, A. V. Dobrynin, *Macromolecules* **2015**, *48*, 5006.